JCTC Journal of Chemical Theory and Computation

Letter

pubs.acs.org/JCTC

Disfavoring Mechanochemical Reactions by Stress-Induced Steric Hindrance

Martin Krupička*,† and Dominik Marx*

Lehrstuhl für Theoretische Chemie, Ruhr-Universität Bochum, 44780 Bochum, Germany

Supporting Information

ABSTRACT: Mechanochemical activation of covalent bonds using sonication, force spectroscopy, or molecular force probes usually lowers activation energies and thus accelerates reactions. However, applying mechanical forces to complex molecules is known to not only stretch covalent bonds but also to distort the molecular skeleton that hosts the activated bonds—leading to nonmonotonous behavior as a function of force. Here, the Bell—Taft model is introduced and validated which both rationalizes and quantifies such nonlinear effects on activation energies, including the transition from catch bonds at low forces to slip binding, in terms of steric hindrance caused by force-induced conformational distortions. The fully parametrized version of the model relies exclusively on readily accessible zero-force data and thus allows one to qualitatively explore mechanically induced reactivity changes in complex setups.

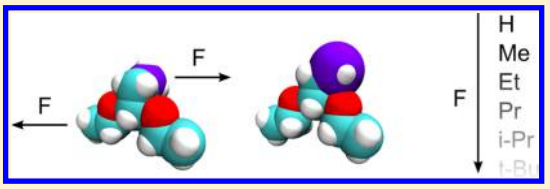

According to textbook knowledge S_N2 reactions are strongly influenced by the steric demand of substituents, which can dramatically decelerate reactions. A long time ago, such effects have been quantified within the framework of linear free energy relationships in terms of Taft's equation.[1−4] Within the emerging field of mechanochemistry[5−7] it is now experimentally established that chemical reactions can be *accelerated* upon exerting mechanical forces.[8−12] Here, we provide several examples for systematic *deceleration* instead and show that the widely used Bell model[13] to quantify mechanochemical activation can be most fruitfully combined with Taft's equation to quantify force-induced steric hindrance. Importantly, this offers a fundamental explanation of the observation of transiently *increasing* barriers as a function of force, i.e. mechanochemical *deactivation*, in terms of force-induced conformational change. Beyond providing a unifying and predictive framework, application to polyethylene glycol (PEG) demonstrates the broad-banded applications.

The selective activation of chemical bonds by mechanical forces, dubbed covalent mechanochemistry (CMC), has seen an explosion of activities due to major advances in force-clamp,[9,14] sonication,[8,10,15] and molecular force probe[11,16,17] techniques. In CMC, the well-documented main effect of mechanical forces on chemical reactions is to *activate* them by *decreasing* activation barriers thus *accelerating* the reaction.[5−7] More recently, however, there is unambiguous evidence accumulating in the literature,[18−24] including direct experimental support,[20,21,23] which clearly shows that tensile stress can also *increase* activation barriers of covalent chemical reactions. Such force-induced bond strengthening has been found about a decade ago for biologically important noncovalent interactions as probed by external forces in the pN range.[25] This so-called catch binding with a subsequent transition to a slip bond beyond a critical force can be modeled in terms of competing reaction channels with different sensitivity to force, possibly combined with different reactant stabilities, or due to local deformations up to large-scale conformational changes in the protein as a result of mechanical strain.[25] Later, such rollover behavior has also been found within CMC for conrotatory ring-opening of benzocyclobutenes in the case of sufficiently long chains.[18] Clearly, such nonlinear behavior of activation energies as a function of force requires models that go beyond Bell's model,[13] which is linear in the applied force. Within CMC, the idea of a Taylor expansion up to quadratic order in the mechanical force term[16] leads to what is called extended Bell theory (EBT).[19,26] The EBT model been shown to correctly predict force-induced deactivation and subsequent rollover to slip binding at higher forces for certain unimolecular covalent reactions.[19,21]

Here, a complementary viewpoint based on the concept of steric hindrance is exploited to understand, model, and predict nonmonotonous chemical reactivity as a function of mechanical pulling, in particular for bimolecular reactions. The reason is that increasing activation barriers can be induced by steric hindrance: a reaction becomes less favorable upon introducing more bulky substituents.[1−4,27−29] For instance, S_N2 reactions are strongly influenced by the steric demand of the substituent, given that attacking nucleophile, reactive carbon, and leaving group should be collinear.[2,29] These effects have been successfully quantified in terms of Taft's equation[1−4] which, therefore, might be an ideal testing ground to explore if force-induced steric hindrance can explain nonmonotonous reactivity as a function of tensile stress. Indeed, using computational models that have been simplified as much as possible we demonstrate that force-induced steric hindrance—triggered by intramolecular conformational changes as a result of stretching

Received: November 26, 2014
Published: February 13, 2015

DOI: 10.1021/ct501058a
J. Chem. Theory Comput. 2015, 11, 841−846

the molecule by mechanical forces—offers a convincing concept to explain and to predict this nonmonotonous mechanochemical phenomenon for S_N2 reactions. Such conformational distortions become effective at low forces only since torsions are the softest degrees of freedom and thus respond readily to sub-nano-Newton forces. Thus, noncovalent[25] and covalent mechanochemistry[5−7] become intimately intertwined in cases where conformational changes counteract mechanical work.

We now introduce a simple yet rich model to study the antagonism of steric deactivation and mechanical activation of generic S_N2 reactions, which is the self-exchange reaction of ethyl propyl ether with ethoxide anion as the nucleophile, see reaction **1** in Figure 1. The molecule is isotentionally[30]

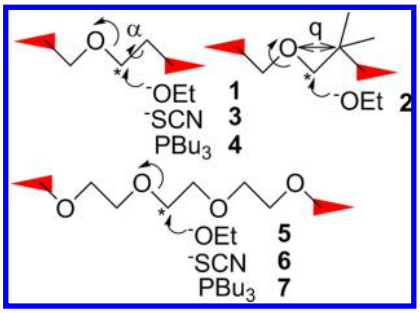

Figure 1. Definition of the substitution reactions investigated under tensile stress showing ethyl propyl ether **1** and ethyl neopentyl ether **2**, where constant collinear forces are applied to the carbon sites (thus being the "pulling points", marked by red arrows) in order to stretch the molecules while being attacked at C*; by an ethoxide anion serving as nucleophile. The dihedral angle α discussed in the text is the O−C*−C−C angle as indicated. Ethyl propyl ether attacked by thiocyanate **3** and tributylphosphine **4** as well as corresponding PEG model reactions **5**, **6**, and **7**.

stretched upon applying collinear forces of opposite direction to its terminal carbon sites (marked by the red arrows). The structures of reactant and transition states (RS, TS) were optimized as a function of constant force and the (corresponding "rigorous") activation energies, $\Delta E^{\ddagger}(F)$, thereby obtained are depicted in Figure 2.

Most surprisingly, we observe in Figure 2(a) a pronounced nonmonotonous behavior at low forces for ethyl propyl ether: up to roughly 0.5 nN the activation barrier *increases* before the expected linear decrease takes over in the nano-Newton regime, i.e. beyond 1 nN (cf. "propyl free" data). Such unexpected behavior cannot be described using Bell's model,[13] which has been shown to perform exceptionally well at sub-nano-Newton forces.[7,19,26,30] Aiming at understanding this observation we searched for additional degrees of freedom that might be the reason for the nonmonotonous change of $\Delta E^{\ddagger}(F)$. By inspection of reaction pathways as a function of external force, we discovered a significant change of the dihedral angle α at the TS, see green data in Figure 2(b). Indeed, α increases already in the sub-nano-Newton regime from about 90 to 180° upon stretching. This readily suggests a deep connection to the concept of steric hindrance, albeit force-induced and not due to chemical substitutions as traditionally.

Stimulated by this observation, we investigated a reference system where α is expected to remain constant and close to 180°, the ethyl neopentyl ether system **2**. First of all, the increased steric hindrance at the TS between the attacking oxygen site and the closest pulled carbon site (symbolized schematically using two half circles in the upper inset of Figure

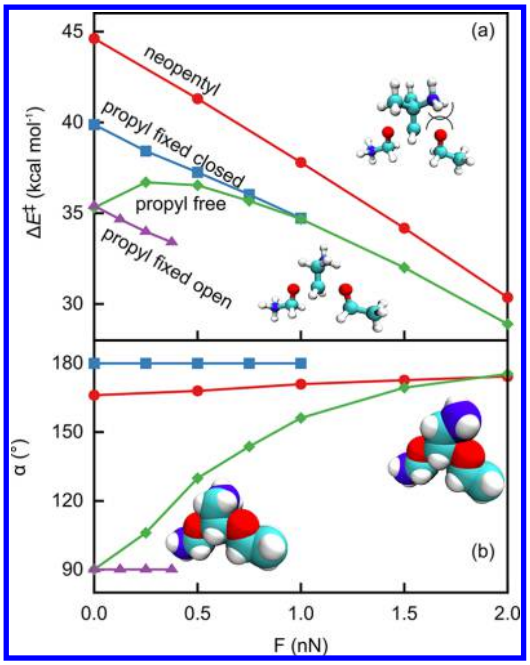

Figure 2. Nonlinear versus linear dependencies of the activation energy as a function of the external mechanical force. Activation energy $\Delta E^{\ddagger}(F)$ in panel (a) and dihedral angle α (see Figure 1) at the TS in panel (b) obtained from isotensional optimization as a function of force for the different model systems as defined and color-coded in the figure. The fully isotensionally optimized ethyl propyl ether reactant is denoted by "free", whereas data from constrained isotensional optimizations are denoted by "fixed closed" and "fixed open" for α = 180 and 90, respectively. The upper and lower insets in (a) show the TS of the neopentyl **2** and propyl **1** systems, respectively, at 0 nN using ball-and-stick representations, whereas the left and right insets in (b) show the TS of the propyl system **1** at 0 and 2 nN, respectively, using van der Waals sphere representations; the two terminal carbon atoms on which the force acts are highlighted using blue spheres.

2(a)) leads, already at zero force, to an increase of activation energy compared to the much less bulky ethyl propyl reactant **1**; see Supplementary Figure 2 for selected TS structures. More importantly, as seen in Figure 2 (red data), this increased activation energy decreases again linearly, as expected according to Bell's model,[13] and the dihedral angle stays not far from 180° in the entire force range studied as a result of having introduced the *tert*-butyl group (being a bulky substituent which imposes steric hindrance that is independent of the dihedral angle α).

To prove our conjecture, two hypothetical conformers were designed by constraining (while stretching) the crucial dihedral angle to what we call closed (α = 180°) and open (α = 90°) for nucleophilic attack. Figure 2(a) indeed confirms that force-induced changes of the torsional mode are directly coupled to the activation energy. In the closed case, disfavoring collinear attack, the activation energy increases significantly in the zero force (thermal) limit, thus heralding steric hindrance, and from there decreases linearly as a function of force. The case where the conformation is constrained at its preferred value of 90°, also features a Bell-like monotonous decrease of the barrier, but of course starting at the fully relaxed value at F = 0 nN.

The uncovered phenomena clearly call for a mechanistic description. The linearly decreasing activation energy of the closed ethyl propyl system (α = 180°) is perfectly described using Bell's phenomenological model, $\Delta E^{\ddagger}_{\mathrm{Bell}}(F) = \Delta E^{\ddagger}_0 - F\Delta\xi$,

DOI: 10.1021/ct501058a
J. Chem. Theory Comput. 2015, 11, 841−846

where $\Delta E_0^{\ddagger}$ is the thermal activation barrier (at F = 0 nN), see Figure 3(a). The parameter $\Delta\xi$ = +0.41 Å, being a constant for

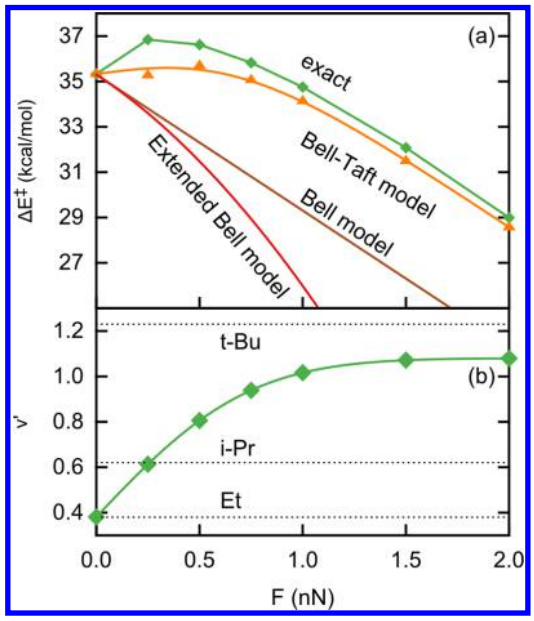

Figure 3. Comparison of the Bell–Taft model to isotensional reference data. Activation energies (a) for ethyl propyl ether reacting with ethoxide where Bell, extended Bell (see text), and Bell–Taft models (where the solid line is obtained using the fully parametrized model, see text and panel b) are compared to the rigorously calculated isotensional reference data ("exact") from Figure 2. The modified steric parameter $\nu'_{ET}(\alpha)$ underlying the Bell–Taft model is shown in panel (b) as a function of force; symbols are data according to eq 2 and solid line is the fully parametrized curve when using eq 3 in eq 2. For comparison experimental[4] ν'_{x0} values (at F = 0 nN) are shown as horizontal dotted lines for x = Et, *i*-Pr, and *t*-Bu.

a given reaction, is determined from these (blue) data and represents the sensitivity of the underlying reaction to tensile force. Next, considering the (green) data in Figure 2, it is clear that the observed nonlinear behavior of $\Delta E^{\ddagger}(F)$ of the unconstrained ethyl propyl system is caused by force-induced changes in steric hindrance.

Based on the success of the nonlinear EBT model to predict force-induced rollover from catch to slip bonds for unimolecular reactions based on zero-force data, we computed the second order term, $\Delta E^{\ddagger}_{EBT}(F) = \Delta E_0^{\ddagger} - F\Delta\xi - (1/2)F^2\Delta\chi$, being the change in compliance $\Delta\chi \approx 0.046$ nm/nN, following the established formalism;[19,21,26] accordingly, here $\Delta\xi$ = +0.418 Å is computed from the change of the distance between the pulling points (marked in Figure 1) when moving from the RS to the TS structure optimized in the absence of force. The results, which are compared in Figure 3(a) to the isotensional benchmark data, demonstrate that this nonlinear extension of Bell's model is unable to capture the more global effects due to force-induced conformational distortions that become effective during this bimolecular substitution reaction.

This raises the question if one can quantify the nonmonotonous force-induced conformational effects on $\Delta E^{\ddagger}$ by explicitly incorporating steric hindrance? An empirical connection of $\Delta E^{\ddagger}$ to the steric demand of substituents is provided by Taft's equation,[31] employing here the formulation by Charton for S_N2 reactions.[4] We thus propose to generalize Bell's model by incorporating Taft's steric term

$$\Delta E^{\ddagger}_{\text{Bell–Taft}}(F) = \Delta E_0^{\ddagger} - F\Delta\xi - 2.303RT\psi'\nu'_x \quad (1)$$

taking the dimensionless parameter ψ' from experiment without any adjustment (cf. reaction set 8 in ref 4); note that 2.303 comes from converting to the natural logarithm. Next, we consider Taft's parameter ν'_x to be conformation-dependent using the simplest possible ansatz

$$\nu'_x(\alpha) = \nu'_{x0} + \eta\cos(\alpha) \quad (2)$$

being a function of the torsional angle α. Here, $\nu'_{x0} = \nu'_{ET}$ = 0.38 is the usual Taft value for the ethyl substituent again taken straight from experiment.[4] At zero force, the optimal angle, here α_0 = 90°, recovers the thermal limit, i.e. $\nu'_x(\alpha_0) = \nu'_{x0} = \nu'_{ET}$. Note that in general a trivial phase shift might be required to ensure cos (α_0) = 0 in the thermal reference and that higher-order Fourier components could be added to eq 2 if required.

The proposed Bell–Taft equation, i.e. eq 1 together with eq 2, extends the model beyond one dimension (as described by the reaction coordinate ξ) by adding the torsion α but contains only one additional parameter. The dimensionless parameter η, which captures the increasing steric hindrance due to changing α, was obtained by fitting to the calculated activation energies of the unconstrained ethyl propyl system, yielding η = 0.70 and the $\nu'_x(F)$ data points in Figure 3(b); while keeping the same $\Delta\xi$ value as before. In stark constrast to Bell's model, the intricate dependence of the activation energy on the external force, including the nonlinear behavior, is qualitatively reproduced by our Bell–Taft model, see Figure 3(a). A remaining caveat is that the force-induced change of the decisive structural variable α, and thus the force-dependence of $\nu'_x(\alpha)$ according to eq 2, still needs to be determined from explicit isotensional optimizations. However, $\alpha(F)$ as depicted in Figure 2(b) can be faithfully represented by

$$\alpha(F) = \alpha_0 + (\alpha_{max} - \alpha_0)\,\text{erf}[F{\cdot}p] \quad (3)$$

with p = 0.773 nN^{-1} for α_0 = 90° and α_{max} = 180°. This dependence finally turns $\nu'_x(\alpha)$ into our fully parametrized force-dependent Taft parameter, see the continuous $\nu'_x(F)$ curve in Figure 3(b), to be used in eq 1 to predict $\Delta E^{\ddagger}_{\text{Bell–Taft}}(F)$ without any finite-force calculation.

Interestingly, the value of the generalized Taft parameter at 2 nN of the stretched propyl system **1** is close to the usual zero-force Taft parameter due to a *t*-Bu group (see the topmost dotted horizontal line in Figure 3(b)) corresponding to the neopentyl system **2**. The same is true for the dihedral angle α of the stretched propyl system at 2 nN, which is essentially identical to that of the neopentyl system at 0 nN, see Figure 2(b). This implies that stretching the propyl system up to 2 nN induces sterical hindrance that corresponds roughly to that caused by introducing a *t*-Bu group at F = 0 nN. This is visualized by inspecting together the four insets in Figure 2, where one can see pictorially that the blue carbon site closest to the attacking oxygen is distorted at 2 nN so much toward this oxygen for **1** (compare the right inset in Figure 2(b) to the left one at F = 0 nN) as found for neopentyl at zero force (see top inset in Figure 2(a)). Indeed, the respective distance at the TS is reduced from about 3.34 Å for **1** at zero force to ≈2.88 Å at 2 nN, which is close to the neopentyl value of roughly 2.71 Å at 0 nN (and even closer after stretching neopentyl up to 2 nN, namely ≈2.87 Å). Our approach thus yields a consistent picture of describing and quantifying the force-induced transition from catch bond behavior to slip binding in terms of stress-induced conformational change that leads to steric hindrance.

DOI: 10.1021/ct501058a
J. Chem. Theory Comput. 2015, 11, 841–846

Encouraged by these results, we strived to assess the transferability of our Bell–Taft model to different nucleophiles, i.e. reactions **3** and **4**, to assess its predictive power. However, Bell's empirical parameter $\Delta\xi$ depends also on the nucleophile. Boulatov and co-workers[32,33] proposed the difference of the distance of a spectator atom to the leaving group (see q in Figure 1) between transition and reactant state *at zero force*, i.e. $\Delta q = q_{TS} - q_{RS}$, to reduce finite-force to zero-force behavior upon using $\Delta\xi \approx \Delta q$. Indeed, we confirm a linear correlation, $\Delta\xi \approx 2\Delta q$, as obtained from our rigorous finite-force data (see the SI). Using this modified Boulatov approximation for $\Delta\xi$ and the same parameters as for the prototypical self-exchange reaction together with the standard experimental values for these nucleophiles,[4] the resulting force-dependent activation energies are depicted in Figure 4(a); note that the same

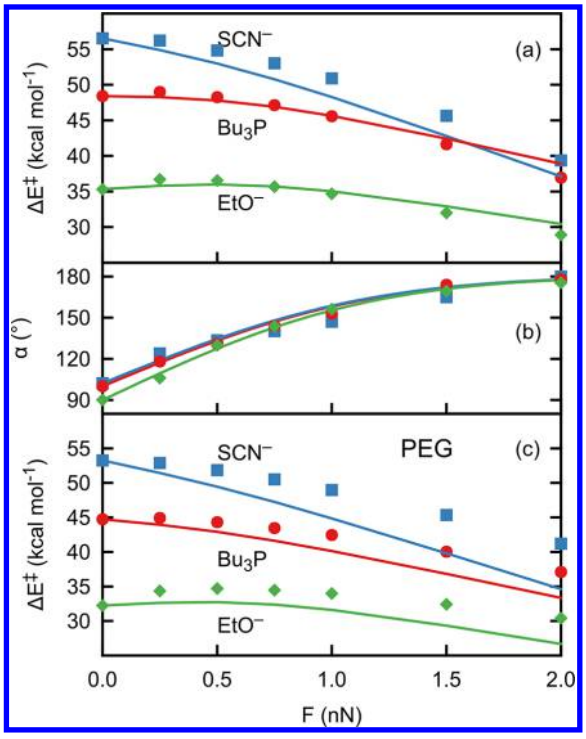

Figure 4. Validation and applications of the Bell–Taft model. Activation energies (a) for reactions **1**, **3**, and **4** as defined and color-coded in the figure, where the symbols represent the rigorous isotensional reference data, whereas the lines show the fully parametrized Bell–Taft model, $\Delta E^{\ddagger}_{\text{Bell–Taft}}(F)$ including the modified Boulatov approximation for $\Delta\xi$. In panel (b) the exact force-induced change of the dihedral angle α corresponding to the systems in (a) is compared to the parametrization based on eq 3 using color-coded symbols and lines, respectively. Panel (c) depicts the rigorous and Bell–Taft activation energies for the three PEG reactions **5**, **6**, and **7** in analogy to panel (a).

parametrization of $\alpha(F)$ as before, eq 3 with α_0 optimized in the absence of force, holds as demonstrated by panel (b). The results are most encouraging: the Bell–Taft model is indeed able to describe the nonlinearity of the force-induced changes of the activation barrier without performing finite-force calculations—much as Taft's equation is able to quantify substituent-induced steric hindrance in the absence of force.

What is, however, the influence of mechanical stretching on the nucleophilic substitution mechanism itself? The More O'Ferrall–Jencks diagram,[34−36] spanned by the distances from the reactive carbon to the leaving group, r(C–LG), and to the attacking nucleophile, r(C–Nuc), reveals that the external force shifts the TS systematically away from its zero-force value toward the lower-left direction according to Figure 5. This

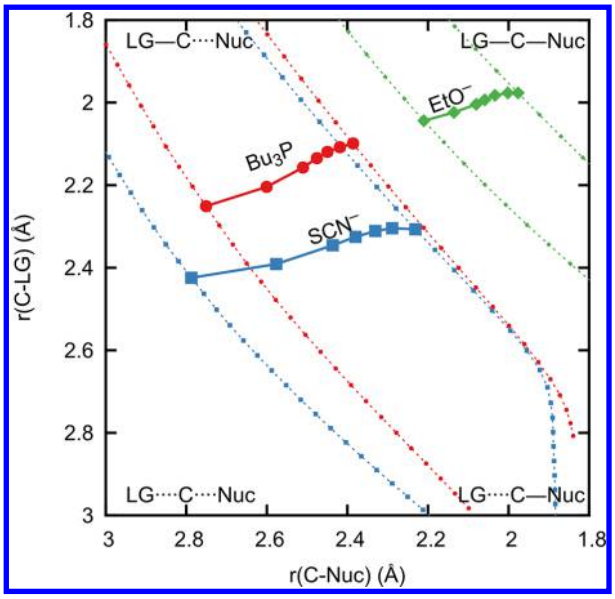

Figure 5. Explanation of the force-induced changes of nucleophilic substitution mechanisms. Force-dependent More O'Ferrall–Jencks analysis of the isotensionally optimized TS structures of **1**, **2**, and **3** at 0.0, 0.25, 0.5, 0.75, 1.0, 1.5, and 2.0 nN (large color-coded symbols linearly connected by solid lines; the respective zero-force data are located at the upper right ends). For each system the corresponding intrinsic reaction coordinate passing through the TS is shown (only) at 0 and 2 nN by small color-coded symbols linearly connected by dotted lines.

implies that the force exerts two distinct effects on the mechanism: the usual Hammond shift along the intrinsic reaction coordinate (IRC) and a mechanical work shift away from the IRC toward the S_N1 regime due to force-induced distortions of the TS structures. Asymptotically the mechanism turns out to be S_N1-like: the leaving group will be torn off and then the carbocation captured by the nucleophile.

Finally, we apply our framework to an interesting problem, namely cleavage of stretched PEG, being routinely used as a force-transducing polymer in CMC experiments.[5−7] The Bell–Taft model was applied without any adjustment to the three PEG reactions **5**, **6**, and **7**. The results in Figure 4(c) show that important trends are qualitatively reproduced by this model that does not require a single finite-force calculation. This opens the door to use the Bell–Taft model to efficiently explore nonmonotonous changes of reactivity due to mechanical activation of complex systems by exclusively using zero-force information as it can be most readily obtained from any standard quantum chemistry package. In particular, the mechanism of the force-induced transition from catch binding to slip bond behavior beyond a critical force described here for bimolecular nucleophilic substitution reactions resembles the phenomenological bond-deformation model in noncovalent mechanochemistry.[25] *En passant*, the Bell–Taft model also provides Taft's parameter ν'_x as a function of dihedral angle. This allows one to directly estimate steric hindrance effects also in systems where the reactive conformation is not distorted by

DOI: 10.1021/ct501058a
J. Chem. Theory Comput. 2015, 11, 841–846

extrinsic forces but rather intrinsically imposed by the molecular skeleton.

In conclusion, bringing together hitherto disconnected concepts from mechanochemistry and steric hindrance upon introducing what we call the Bell−Taft model, we are able to quantify mechanochemical *deactivation* effects observed in the sub-nano-Newton force regime and subsequent rollover to activation beyond a critical force. At such low forces, where mainly the soft conformational degrees of freedom are affected, steric hindrance can be increased easily as a result of molecular adaptation to the external force. The similar magnitude of mechanical distortion and steric hindrance only in the low force regime explains that this antagonistic effect can result in roughly force-independent activation energies therein. Since conformational distortions are inevitable when nonrigid molecules are exposed to tensile stress, be it via sonication of polymer-functionalized mechanophores[10,37] or in force-clamp experiments on enzymes,[38,39] we expect this fundamental concept and the qualitative Bell−Taft model to be of widespread importance in chemistry and biochemistry.

METHODS

The static quantum chemical calculations were performed using a well-established implicit solvation model (IEFPCM[40]) together with the robust B3LYP density functional and the 6-31+G(d) basis set as implemented in Gaussian 09.[41] The calculations have been performed using our in-house modified Gaussian 09 code to carry out rigorously isotensional optimizations,[30] where constant collinear forces have been applied to the marked carbon sites as sketched in Figure 1. At each value of the constant force, the RS and TS structures of the reactive complex have been optimized in continuum solvent either completely or upon applying additional constraints on α as descibed in the text.

ASSOCIATED CONTENT

Supporting Information

Additional analyses and coordinates. This material is available free of charge via the Internet at http://pubs.acs.org.

AUTHOR INFORMATION

Corresponding Authors

*E-mail: martin.krupicka@theochem.rub.de.
*E-mail: dominik.marx@rub.de.

Present Address

†Max-Planck-Institut für Chemische Energiekonversion, Stiftstrasse 34-36, 45470 Mülheim an der Ruhr, Germany.

Notes

The authors declare no competing financial interest.

ACKNOWLEDGMENTS

We gratefully acknowledge financial support by the Reinhart Koselleck Grant "Understanding Mechanochemistry" (DFG MA 1547/9). The calculations were carried out using resources from NIC Jülich, BOVILAB@RUB, and Rechnerverbund-NRW.

REFERENCES

(1) Taft, R. W. *J. Am. Chem. Soc.* **1952**, *74*, 3120−3128.
(2) Gallo, R. *Prog. Phys. Org. Chem.* **1983**, *14*, 115−163.
(3) Williams, A. *Free Energy Relationships in Organic and Bio-organic Chemistry*; The Royal Society of Chemistry: Cambridge, 2003.
(4) Charton, M. *J. Am. Chem. Soc.* **1975**, *97*, 3694−3697.
(5) Beyer, M. K.; Clausen-Schaumann, H. *Chem. Rev.* **2005**, *105*, 2921−2948.
(6) Caruso, M. M.; Davis, D. A.; Shen, Q.; Odom, S. A.; Sottos, N. R.; White, S. R.; Moore, J. S. *Chem. Rev.* **2009**, *109*, 5755−5798.
(7) Ribas-Arino, J.; Marx, D. *Chem. Rev.* **2012**, *112*, 5412−5487.
(8) Paulusse, J. M. J.; Sijbesma, R. P. *Angew. Chem., Int. Ed.* **2004**, *43*, 4460−4462.
(9) Wiita, A. P.; Ainavarapu, S. R. K.; Huang, H. H.; Fernandez, J. M. *Proc. Natl. Acad. Sci. U. S. A.* **2006**, *103*, 7222−7227.
(10) Hickenboth, C. R.; Moore, J. S.; White, S. R.; Sottos, N. R.; Baudry, J.; Wilson, S. R. *Nature* **2007**, *446*, 423−427.
(11) Yang, Q.-Z.; Huang, Z.; Kucharski, T. J.; Khvostichenko, D.; Chen, J.; Boulatov, R. *Nat. Nanotechnol.* **2009**, *4*, 302−306.
(12) Wu, D.; Lenhardt, J. M.; Black, A. L.; Akhremitchev, B. B.; Craig, S. L. *J. Am. Chem. Soc.* **2010**, *132*, 15936−15938.
(13) Bell, G. I. *Science* **1978**, *200*, 618−627.
(14) Liang, J.; Fernández, J. M. *ACS Nano* **2009**, *3*, 1628−1645.
(15) Cravotto, G.; Cintas, P. *Angew. Chem., Int. Ed.* **2007**, *46*, 5476−5478.
(16) Huang, Z.; Boulatov, R. *Pure Appl. Chem.* **2010**, *82*, 931−951.
(17) Akbulatov, S.; Tian, Y.; Boulatov, R. *J. Am. Chem. Soc.* **2012**, *134*, 7620−7623.
(18) Dopieralski, P.; Anjukandi, P.; Rückert, M.; Shiga, M.; Ribas-Arino, J.; Marx, D. *J. Mater. Chem.* **2011**, *21*, 8309−8316.
(19) Bailey, A.; Mosey, N. J. *J. Chem. Phys.* **2012**, *136*, 044102−11.
(20) Akbulatov, S.; Tian, Y.; Kapustin, E.; Boulatov, R. *Angew. Chem., Int. Ed.* **2013**, *52*, 6992−6995.
(21) Konda, S. S. M.; Brantley, J. N.; Varghese, B. T.; Wiggins, K. M.; Bielawski, C. W.; Makarov, D. E. *J. Am. Chem. Soc.* **2013**, *135*, 12722−12729.
(22) Tian, Y.; Kucharski, T. J.; Yang, Q.-Z.; Boulatov, R. *Nat. Commun.* **2013**, *4*, 2538.
(23) Groote, R.; Szyja, B. M.; Leibfarth, F. A.; Hawker, C. J.; Doltsinis, N. L.; Sijbesma, R. P. *Macromolecules* **2014**, *47*, 1187−1192.
(24) Krupicka, M.; Sander, W.; Marx, D. *J. Phys. Chem. Lett.* **2014**, *5*, 905−909.
(25) Prezhdo, O. V.; Pereverzev, Y. V. *Acc. Chem. Res.* **2009**, *42*, 693−703 PMID: 19331389.
(26) Konda, S. S. M.; Brantley, J. N.; Bielawski, C. W.; Makarov, D. E. *J. Chem. Phys.* **2011**, *135*, 164103−8.
(27) MacPhee, J. A.; Panaye, A.; Dubois, J.-E. *Tetrahedron* **1978**, *34*, 3553−3562.
(28) Dubois, J.-E.; Macphee, J. A.; Panaye, A. *Tetrahedron* **1980**, *36*, 919−928.
(29) Caldwell, G.; Magnera, T. F.; Kebarle, P. *J. Am. Chem. Soc.* **1984**, *106*, 959−966.
(30) Ribas-Arino, J.; Shiga, M.; Marx, D. *Angew. Chem., Int. Ed.* **2009**, *48*, 4190−4193.
(31) Taft, R. W. *J. Am. Chem. Soc.* **1953**, *75*, 4538−4539.
(32) Kucharski, T. J.; Yang, Q.-Z.; Tian, Y.; Boulatov, R. *J. Phys. Chem. Lett.* **2010**, *1*, 2820−2825.
(33) Tian, Y.; Boulatov, R. *Chem. Commun.* **2013**, *49*, 4187−4189.
(34) More O'Ferrall, R. A. *J. Chem. Soc. B* **1970**, 274−277.
(35) Jencks, W. P. *Chem. Rev.* **1972**, *72*, 705−718.
(36) Harris, J. M.; Shafer, S. G.; Moffatt, J. R.; Becker, A. R. *J. Am. Chem. Soc.* **1979**, *101*, 3295−3300.
(37) Ribas-Arino, J.; Shiga, M.; Marx, D. *J. Am. Chem. Soc.* **2010**, *132*, 10609−10614.
(38) Garcia-Manyes, S.; Liang, J.; Szoszkiewicz, R.; Kuo, T.-L.; Fernández, J. M. *Nat. Chem.* **2009**, *1*, 236−242.
(39) Dopieralski, P.; Ribas-Arino, J.; Anjukandi, P.; Krupicka, M.; Kiss, J.; Marx, D. *Nat. Chem.* **2013**, *5*, 110−114.
(40) Scalmani, G.; Frisch, M. J. *J. Chem. Phys.* **2010**, *132*, 114110−15.
(41) Frisch, M. J.; Trucks, G. W.; Schlegel, H. B.; Scuseria, G. E.; Robb, J. R., Cheeseman, M. A.; Scalmani, G.; Barone, V.; Mennucci, B.; Petersson, G. A.; Nakatsuji, H.; Caricato, M.; Li, X.; Hratchian, H. P.; Izmaylov, A. F.; Bloino, J.; Zheng, G.; Sonnenberg, J. L.; Hada, M.; Ehara, M.; Toyota, K.; Fukuda, R.; Hasegawa, J.; Ishida, M.; Nakajima,

DOI: 10.1021/ct501058a
J. Chem. Theory Comput. 2015, 11, 841−846

T.; Honda, Y.; Kitao, O.; Nakai, H.; Vreven, T.; Montgomery, J. A., Jr.; Peralta, J. E.; Ogliaro, F.; Bearpark, M.; Heyd, J. J.; Brothers, E.; Kudin, K. N.; Staroverov, V. N.; Kobayashi, R.; Normand, J.; Raghavachari, K.; Rendell, A.; Burant, J. C.; Iyengar, S. S.; Tomasi, J.; Cossi, M.; Rega, N.; Millam, J. M.; Klene, M.; Knox, J. E.; Cross, J. B.; Bakken, V.; Adamo, C.; Jaramillo, J.; Gomperts, R.; Stratmann, R. E.; Yazyev, O.; Austin, A. J.; Cammi, R.; Pomelli, C.; Ochterski, J. W.; Martin, R. L.; Morokuma, K.; Zakrzewski, V. G.; Voth, G. A.; Salvador, P.; Dannenberg, J. J.; Dapprich, S.; Daniels, A. D.; Farkas, Ã.; Foresman, J. B.; Ortiz, J. V.; Cioslowski, J.; Fox, D. J. *Gaussian 09, Revision C.01*; 2009.

DOI: 10.1021/ct501058a
J. Chem. Theory Comput. 2015, 11, 841−846